Precision Imaging and Control for Machine Vision Research at Carnegie Mellon University

Reg G. Willson and Steven A. Shafer

March 1992
CMU-CS-92-118

School of Computer Science
Carnegie Mellon University
Pittsburgh, Pennsylvania 15213

Appeared in the *Proceedings of the SPIE Conference on High Resolution Sensors and Hybrid Systems*, February 10-14, 1992 San Jose, CA.

This research was sponsored by the Avionics Laboratory, Wright Research and Development Center, Aeronautical Systems Division (AFSC), U. S. Air Force, Wright-Patterson AFB, OH 45433-6543 under Contract F33615-90-C-1465, ARPA Order No. 7597. The views and conclusions contained in this document are those of the authors and should not be interpreted as representing the official policies, either expressed or implied, of DARPA or the U.S. Government.

Keywords:
camera calibration, computer vision, automated camera systems, Calibrated Imaging Lab

Contents

1 Multi degree of freedom camera systems **1**

2 Calibrated Imaging Lab **2**
2.1 General facilities 2
2.2 Cosmicar/Panasonic camera system 3
2.3 Fujinon/Photometrics camera system 3
2.4 Lens automation 4
2.5 Summary of computer-controlled camera degrees of freedom 6

3 Multi degree of freedom camera models **7**
3.1 Building a MDOF magnification model 7
3.2 Building a MDOF focussed distance model 11
3.3 Building a MDOF optical axis model 12
3.4 The general calibration approach 14

4 MDOF camera models and machine vision tasks **16**
4.1 MDOF color imaging 16
4.2 MDOF focus ranging 17

5 Conclusions **21**

6 Acknowledgments **22**

List of Figures

1 Motor / lens push rod assembly 5
2 Motor / lens double push rod assembly 5
3 Motor / lens pulley assembly 5
4 Pin hole camera model 8
5 Magnification vs focal length 8
6 Focus magnification 9
7 Magnification vs focus motor 9
8 Magnification vs focus and focal length motors 10
9 Chromatic aberration 10
10 Magnification vs focus distance and color band 10
11 Peak focus position vs focal length 12
12 Peak focus position vs aperture 12
13 Image center for 5 focus distances 13
14 Image center for 3 image bands 13
15 Full field error - conventional (1-DOF) imaging approach 18
16 Full field error - MDOF imaging approach 18
17 Box and bar focus targets 19
18 Focus vs focal length settings for MDOF focusing 19
19 Criterion function peak position vs target type and focus type 20

Abstract

In a perfect world we would be able to use the many possible degrees of freedom in a camera system to do many useful things, such as accommodating for changes or differences in the scenes being imaged, correcting for camera behaviour that isn't quite ideal, or measuring properties of the scene by noting how the scene's image changes as the camera's parameters are varied. Unfortunately the parameters that control the formation of the camera's images often interact in complex and subtle ways that can cause unforeseen problems for machine vision tasks.

To be able to effectively use multi degree of freedom camera systems we need to know how variations in the camera's control parameters are going to cause changes in the produced images. For this we need to have good mathematical models describing the relationships between the control parameters and the parameters of the resulting images. Ideally we would like to base the form of the models on an understanding of the underlying physical processes involved, but in many cases these are either unknown or are just too complex to model. In these situations experimentation and generalized modeling techniques are necessary. To perform the experiments needed to develop and validate models and to obtain calibration data for the models we need precise automated imaging systems.

In this report we describe the camera systems developed for Carnegie Mellon University's Calibrated Imaging Lab and show how these systems have been used to develop methods for using computer-controlled cameras and lenses.

1 Multi degree of freedom camera systems

Camera systems used in computer vision often have multiple degrees of freedom (MDOFs), including for example focal length, focus position, aperture, color filter, shutter time, sensor gain and camera position and orientation. These degrees of freedom allow the user to adapt or match the camera's performance to the imaging requirements of the scene (accommodation), to compensate for non-ideal camera behavior by simulating a simpler system (correction or abstraction), or to extract information from the scene by measuring how an image changes as one or more control parameters are varied (measurement). To be able to effectively use MDOF camera systems we need to know the mathematical relationships between the camera's control parameters and the parameters of the resulting images.

In modeling systems it helps to have an understanding of the underlying physical processes involved. If the processes are straight forward or if they are accessible and can be directly measured then the modeling task can be greatly simplified. This is why it is relatively easy to develop MDOF camera models for the kinematic degrees of freedom (ie. x, y, z, θ_x, θ_y and θ_z). If instead the underlying physical processes are complex or inaccessible then the modeling task can be more difficult. For this reason it is difficult to develop MDOF models for a camera's optical DOFs (ie. focal length, focus distance, aperture and color band). In fact, to date almost all camera modeling and calibration work for machine vision and photogrammetry involves systems that either use no controlled optical DOFs (ie. fixed lenses) or use only one controlled optical DOF (eg. focus).

In modeling MDOF optical systems where there is only a limited understanding of the underlying physical processes extensive experimentation is often necessary to develop the models and to collect calibration data. The Calibrated Imaging Lab at CMU provides a highly controlled environment and precision automated cameras for just these kinds of experiments. In this report we discuss the design considerations and tradeoffs that have gone into the development of the CIL's camera systems and illustrate their use in the development of three MDOF models. Subsequently we show how these models can be effectively used to improve the performance of two low level vision tasks.

This work was originally presented in Willson [9] at the 1992 SPIE Conference on High Resolution Sensors and Hybrid Systems.

2 Calibrated Imaging Lab

The Calibrated Imaging Lab at CMU provides a highly controlled environment for experiments in physics based machine vision, including color interreflection, surface roughness, texture analysis and camera modeling and calibration. The general lab facilities include a light tight imaging area and a variety of lighting, positioning and measurement equipment. The lab also has two high precision automated camera systems developed by us specifically for physics based machine vision research. In this section we briefly describe the general facilities in the lab and then describe the development of the two camera systems and their automated lenses.

2.1 General facilities

The key feature of the Calibrated Imaging Lab is a 21×10×12-foot "imaging studio" that can be sealed off from the computer equipment and other work areas in the room. This studio presents a controllable environment for acquiring image data to support research in machine vision.

The studio area has a black ceiling and black carpet; black curtains are also normally used, to eliminate all reflections from the walls. This allows direct illumination to be configured and modeled relatively easily. There are also white curtains that can be pulled around the entire area for studies of diffuse illumination (shadows, etc.).

Lighting facilities include a battery of six MacBeth multi-spectral fixtures for diffuse lighting by three different sources (incandescent or cool or warm fluorescent). For directional lighting, the lab has several 1000W theater spotlights hung from a grid of pipework on the ceiling. For many purposes, free-standing 600W photographers' lights are used with manually operated dimmers.

The lab features an optical table used for placing objects to be viewed. On this table is a large (60-inch) travel rail table fitted with an 8-inch diameter 360-degree Daedal rotation platform. Test targets and objects of various types are placed on the platform for stationery imaging or controlled motion.

For moving the camera, the lab has a full 6-DOF rotation/translation jig that moves a 12×18-inch platform with high precision (0.001 inch and 0.01 degree resolution). Combined with the rail table, the camera-to-object distance can be varied from about 1m to 3m. The rail table, rotation platform and camera jig are all controlled by the lab's Sun4 workstation.

The CIL also has calibration equipment and targets. For geometric calibration, the lab has a pair of Lietz DT20E 20-arc-second surveyor's theodolites; with these, we can determine the position of any point in the lab with a precision uncertainty of about 0.3mm in each dimension. For radiometric calibration, the lab has a Gamma Scientific spectroradiometer. This is used as a unit for measuring reflectance, transmittance, or illumination; and it can be disassembled for measuring the spectral responsivity properties of a camera. The CIL has numerous commercial test targets such as gray-scale charts; and has designed many additional targets such as the CMU Color Chart, which is particularly well-suited for color cameras used in machine vision.

Taken together, in conjunction with the cameras and lenses describe below, the facilities of the CIL provide an environment for controlled experimentation in a wide variety of topics of machine vision research.

2.2 Cosmicar/Panasonic camera system

The Cosmicar/Panasonic camera system was our first attempt at building a precision camera system. Our objective was to take a conventional CCTV camera system and see what type of performance we could get out of it. The system consists of a Cosmicar CCTV grade zoom lens mounted on a Panasonic GP-MF702 MOS solid state camera. The video signal from the camera is digitized to 8-bits/pixel by a Matrox VIP frame grabber in the lab's Sun4 workstation. To select the color band the system uses a seven slot motorized filter wheel housing six filters, including red, green and blue (Wratten #25, 58 and 47B), 0.3 neutral density, 0.6 neutral density and 0.9 neutral density. As CCD cameras are generally sensitive down well into the infra red and since all of the band pass filters that we use are transparent in the IR regions we use a total IR block (Schott KG5) mounted directly on the camera lens.

While the Panasonic video camera is fairly high quality, the camera's images suffer from the timing jitter and noise problems common to all video cameras [2]. The limited dynamic range of the camera combined with a fixed sensor gain and exposure time make experimentation with the full range of aperture positions very difficult to do. Another shortcoming of the system results from the low sensitivity of the camera in the blue region plus the low light transmission of the blue filter. This necessitates the use of wide apertures to improve the SNR of the blue images during color imaging.

2.3 Fujinon/Photometrics camera system

The Fujinon/Photometrics camera system results from our efforts to improve on the shortcomings of the Cosmicar/Panasonic camera system. The system consists of a Fujinon ENG color camera grade zoom lens mounted on a Photometrics Star I scientific camera. Images are digitized to 12-bits/pixel in the camera head by the camera's controller and then transferred to the lab's host computer over a GPIB interface. To select the color band the system has a built in six slot motorized filter wheel housing five filters, including red, green, blue, 0.3 neutral density and 0.9 neutral density. The system also has an IR block mounted directly on the camera lens.

In the Fujinon/Photometrics system the 2/3-inch image format produced by the lens does not completely cover the camera's sensor array and thus the usable image size for the camera (338×338 pixels) is smaller than the full sensor size. There were several reasons for this tradeoff. First, the Photometrics camera has a relatively large back flange focal length (on the order of 45mm, even with a custom machined camera head). This precludes using commercially available CCTV camera lenses which typically have back flange focal lengths in the range of 10-20mm. Second, in our experience, to be able to precisely motorize the lens body we needed a lens where the focal length DOF was rotational. This eliminated almost all commercially available 35mm format zoom lenses. Of the remaining 35mm format lenses that we examined none had a sufficiently large enough range of focal lengths or a solid enough mechanical movement for our purposes. This left us with commercial ENG/EFP lenses and broadcast quality TV lenses to choose from. For both of these types of lenses the cost of a 1-inch format lens was prohibitive. In the end the Fujinon lens that we chose had the necessary range of focal lengths, three rotational DOFs, robust mechanical movement and a 48mm back flange focal length.

The Fujinon/Photometrics camera has several major advantages over the Cosmicar/Panasonic system. The Photometrics camera features direct pixel by pixel digitization virtually eliminating timing jitter as a source of image noise. In addition the camera is cooled to -40°C which further improves the SNR of the image. The 12-bit dynamic range of the Photometrics camera is also a significant improvement over the Panasonic camera's 8-bit dynamic range. The variable

exposure time and sensor gain of the Photometrics camera gives us an ability to experiment over the full range of aperture values that was unavailable with the Panasonic camera's fixed exposure time and gain. Finally the Fujinon/Photometrics camera was also designed with a larger focal length range and with finer control of the focus and focal length DOFs compared to the Cosmicar/Panasonic camera.

The Fujinon/Photometrics camera system is not without its limitations, however. To minimize the effects of variations in the shutter rise and fall times and to improve the SNR of the images, exposure times typically must be greater than 0.5 seconds for the Photometrics camera. The longer exposure time combined with the 3-4 seconds required to transfer a full image from the camera controller to the lab's workstation results in a relatively slow imaging speed for the camera. In comparison the Cosmicar/Panasonic camera system can image at a rate of 30 frames/second. At $23\times23\mu$m the pixel size for the Photometrics camera is very large and results in aliasing problems in images with high spatial frequency content. The 338×338 pixel effective image size is also a major drawback. Finally, saturation and blooming in the Photometrics camera has proved to be very difficult to control. In conclusion, rather than replace the initial Cosmicar/Panasonic camera system, the Fujinon/Photometrics camera system is used to complement it for high radiometric precision and geometric stability at a cost of speed and spatial resolution.

2.4 Lens automation

The strength of the CIL's camera systems lies in their high precision lens automation. Automation for both the Cosmicar and Fujinon lenses is provided by digital microstepping motors on each of the focal length, focus and aperture DOFs. The nature of the microstepping motors ensures precise drift free repeatability for all of the lens control parameters.

For the Cosmicar lens all three motor shafts are connected to the rotational rings on the lens body by push rod assemblies similar to the one illustrated in Figure 1. This design provides a 1:1 transfer of the motor's angular position to the lens body with virtually no mechanical play.

For the Fujinon lens the larger range of motion for the lens' focus distance ring requires the two push rod assembly illustrated in Figure 2 to minimize the amount of lateral force exerted on the lens body. The two rod design requires an additional motor pivot to compensate for the translation of the lens' focus element along the optical axis, but has the advantage over the single rod approach of transferring a moment between the motor and the lens body rather than a force. The small range of motion for the Fujinon lens' focal length ring combined with the lens' large range of focal length necessitates the stepdown wire pulley arrangement illustrated in Figure 3 to achieve sufficient resolution of the lens magnification. The tensioned pulley design provides a 3.5:1 transfer of the motor's angular position to the angular position of the lens's zoom ring, again with no mechanical play. Finally the aperture of the Fujinon lens is controlled using the single push rod assembly illustrated in Figure 1.

In most zoom lenses the focal length of the lens is changed by moving groups of lens elements relative to one another using internal cams and slides. In our system we minimize the effects of this internal source of mechanical play and any external stepper motor hysteresis by always approaching a desired motor position from one direction.

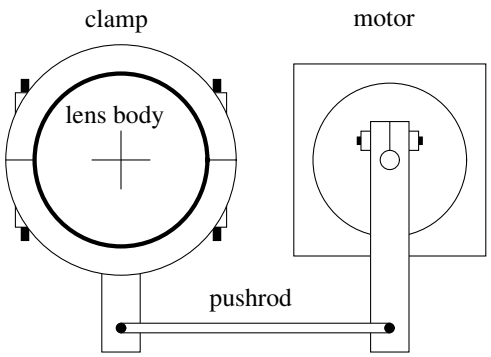

Figure 1: Motor / lens push rod assembly

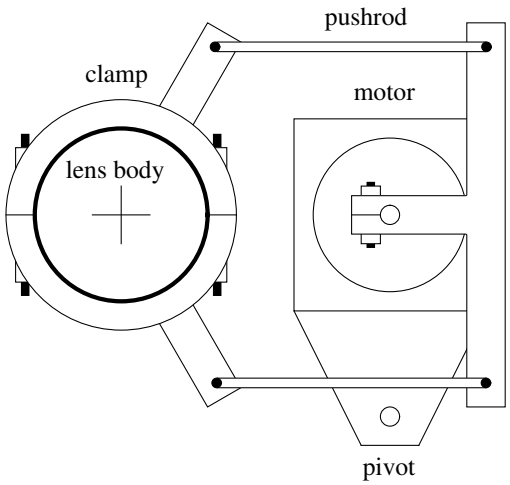

Figure 2: Motor / lens double push rod assembly

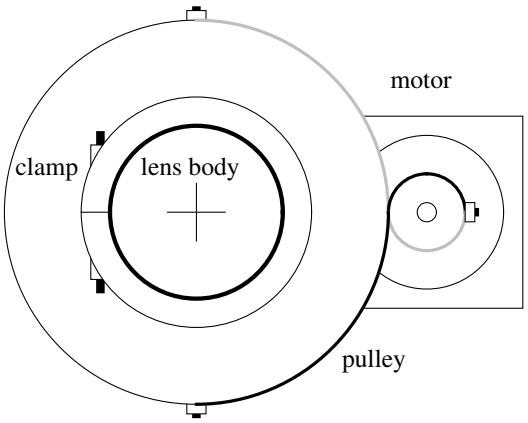

Figure 3: Motor / lens pulley assembly

2.5 Summary of computer-controlled camera degrees of freedom

These two systems - a CCTV system and a scientific camera system - give the CIL precise computer control over the most common camera DOFs. The Cosmicar/Panasonic camera system provides a total of 10 computer-controlled DOFs, listed in the following table.

Cosmicar/Panasonic camera system		
parameter	operating range	control resolution
Focus distance	1.0m - ∞	3900 steps (110° of travel)
Focal length	12.5 - 75mm	4000 steps (113° of travel)
Aperture	F1.8 - closed	2700 steps (76° of travel)
Color band	none,red,green,blue	7 filters
x, y, z	24 in, 12 in, 80 in	0.001 inches
θ_x, θ_y, θ_z	$\pm 20°$, $\pm 20°$, $\pm 10°$	0.01 degrees

The Fujinon/Photometrics camera system provides the same 10 DOFs as the Cosmicar/Panasonic system, plus the ability to set the sensor's gain and exposure time. The automation for the Fujinon lens also has 30% more control resolution in the focus and focal length DOFs.

Fujinon/Photometrics camera system		
parameter	operating range	control resolution
Focus distance	1.0m - ∞	5100 steps (143° of travel)
Focal length	10 - 130mm	11100 steps (89° of travel)
Aperture	F1.7 - closed	2700 steps (76° of travel)
Color band	none,red,green,blue	6 filters
x, y, z	24 in, 12 in, 80 in	0.001 inches
θ_x, θ_y, θ_z	$\pm 20°$, $\pm 20°$, $\pm 10°$	0.01 degrees
Exposure time	0.0 - 6553.6 secs	0.1 seconds
Sensor gain	20 or 5 electrons / ADU	high/low

3 Multi degree of freedom camera models

In MDOF camera systems there is, to a first order approximation, a one to one correspondence between each camera parameter we control (eg. zoom and focus) and a specific parameter of the produced images (eg. image magnification, focussed distance). For the most part machine vision researchers use these first order approximations when constructing and calibrating camera models (eg. pin hole and thin lens camera models). When the camera systems they are modeling have only one controlled DOF then using the first order approximation often works reasonably well. However, when two or more DOFs are varied the effects of the interaction of the controlled parameters on the resulting image parameters must be taken into account.

In this section we look at three image parameters: image magnification, focussed distance and optical axis. For each image parameter we describe the development of a MDOF camera model by starting from a 1-DOF model and augmenting it with any additional control parameters that are found to be significant.

3.1 Building a MDOF magnification model

Image magnification can be defined as the solid angle of the field of view that is subtended by the camera sensor. To a first order approximation the magnification of a camera lens is proportional to the focal length of the lens, ie:

$$M = cf_{length}$$

where c is a constant of proportionality and f_{length} is the effective focal length of the lens. This relationship is embodied in the commonly used pin hole camera model illustrated in Figure 4.

In a real camera system there will almost never be a direct 1:1 relationship between the focal length motor settings and the actual effective focal length of the lens. This is clearly the case for our lens, for which the plot of lens magnification versus the focal length motor can be seen in Figure 5. For this example a reasonable model for this relationship would probably be a simple quadratic function. Combining this with our first order approximation our 1-DOF magnification model can then be expressed as

$$M = c_1 + c_2 f_l + c_3 f_l^2 = g_M(f_l; c_1, c_2, c_3)$$

where

M	is the image magnification,
g_M	is the parameterized model of the control parameter and the calibration coefficients,
f_l	is the focal length motor and
c_1, c_2, c_3	are coefficients to be determined by calibration.

Unfortunately our 1-DOF model doesn't tell the whole story. As anyone who has ever focussed a camera knows, image magnification can also be changed by adjusting the focus of the lens. Figure 7 shows a plot of image magnification as a function of the focus motor of the lens. The change in magnification follows from the physics of the image formation process, illustrated in Figure 6 for a simple thin lens. As the focus of the lens is varied from near to far the magnification of an object located at a fixed distance from the lens decreases.

As the pin hole camera model has no concept of focus there does not seem to be any direct way to augment our existing 1-DOF model with the focus DOF. However, if we use the thin

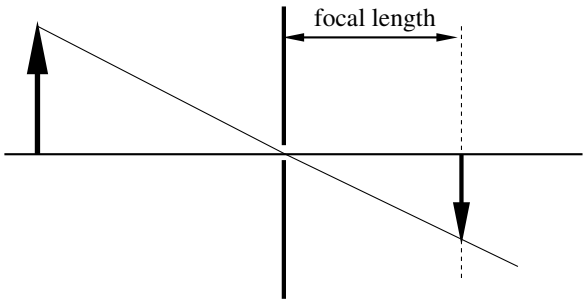

Figure 4: Pin hole camera model

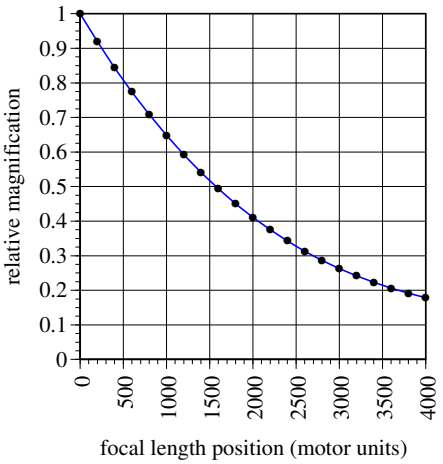

Figure 5: Magnification vs focal length

lens model of the image formation process illustrated in Figure 6 we can see that there is a direct relationship between the focus position of the lens (the separation of the sensor plane and the optical center of the lens) and the image magnification. Thus to augment the 1-DOF model possibly all we need do is multiply it by the focus position of the lens. If we model the relationship between the focus position of the lens and the focus motor with another quadratic function, the resulting 2-DOF magnification model can be expressed as

$$M = (c_1 + c_2 f_l + c_3 f_l^2)(c_4 + c_5 f_d + c_6 f_d^2) = g_M(f_l, f_d; c_1, ..., c_6)$$

where

M	is the image magnification,
g_M	is the parameterized model of the control parameters and calibration coefficients,
f_l	is the focal length motor,
f_d	is the focus motor and
$c_1 ... c_6$	are coefficients determined by calibration.

At this point, when we try to fit the model to magnification data from the lens, we find that the above form for our magnification model doesn't fit that well. This occurs for two reasons. For one, the actual process involved in varying the focal length of a zoom lens really has no relation to the pin hole camera model. The second reason is that the actual relationship between the lens' motor settings and internal lens parameters is generally an arbitrary function chosen by the lens manufacturer and is not necessarily well modeled by a simple quadratic function. To deal with these problems a more generalized modeling technique must be used. In [6] Tarabanis uses table look-up with interpolation to model the relationship between image magnification and the focal length and focus distance control parameters of their lens. In [8] we use bivariate cubic polynomials to model the relationship. Calibration involves performing a least squares fit of the model to collected magnification data to determine the coefficients of best fit for the bivariate polynomials. The resulting 2-DOF magnification model (shown in Figure 8), has the form:

$$M = c_1 + c_2 f_d + c_3 f_d^2 + c_4 f_d^3 + c_5 f_l + c_6 f_l f_d + c_7 f_l f_d^2 + c_8 f_l^2 + c_9 f_l^2 f_d + c_{10} f_l^3 = g_M(f_l, f_d; c_1 ... c_{10})$$

where

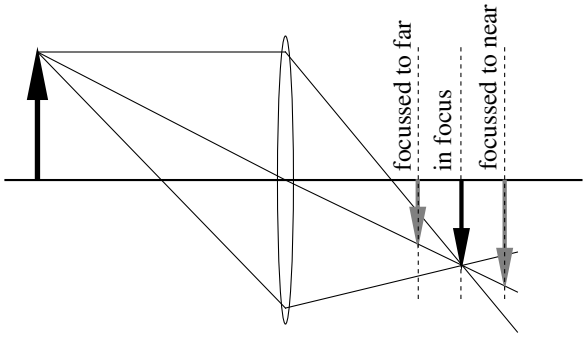

Figure 6: Focus magnification

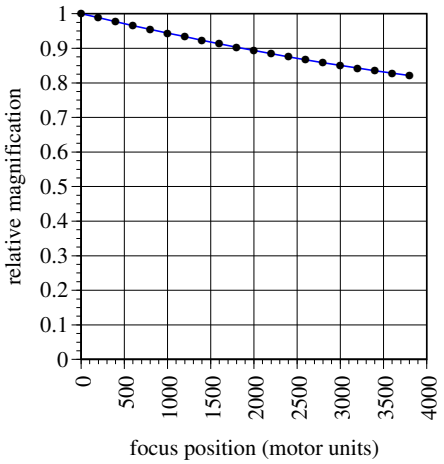

Figure 7: Magnification vs focus motor

M	is the image magnification,
g_M	is the parameterized model of the control parameters and calibration coefficients,
f_l	is the focal length motor,
f_d	is the focus motor and
$c_1 ... c_{10}$	are coefficients determined by calibration.

Our model is still not complete, however. Ideally, the image magnification of the lens would be independent of the wavelength of the light used for the imaging. This is not the case in reality. Lateral chromatic aberration, illustrated in Figure 9, can cause the magnification of images taken in different color bands to differ by as much as 0.5% [8]. Figure 10 shows the image magnification for the red, green and blue bands for several focus motor positions. It would be virtually impossible to find a continuous closed form for the dependence of the magnification on wavelength for a lens. Fortunately, most multi-band imaging systems use only a small fixed number of color filters to vary the imaging wavelength so we can easily add a λ DOF to the model by simply calibrating a separate magnification model in each band with data taken in that color band. Our 3-DOF magnification model now looks like

$$M = g_M(f_l, f_d, \lambda; c_1 ... c_{30})$$

where

M	is the image magnification,
g_M	is the parameterized model of the control parameters and calibration coefficients,
f_l	is the focal length motor,
f_d	is the focus motor,
λ	is the color band, and
$c_1 ... c_{30}$	are coefficients determined by calibration.

The only remaining DOF in the camera system that can potentially have an effect on the image magnification is the aperture. For our lenses, careful measurements of the image magnification show no significant magnification variation with changes in the aperture. If some dependency does exist, it's below our measurement capability. So, we accept the above MDOF model of magnification.

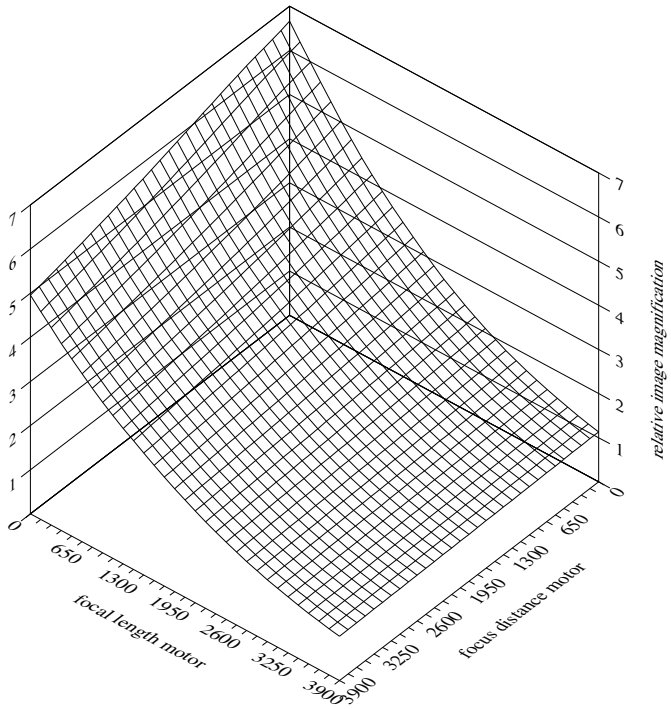

Figure 8: Magnification vs focus and focal length motors

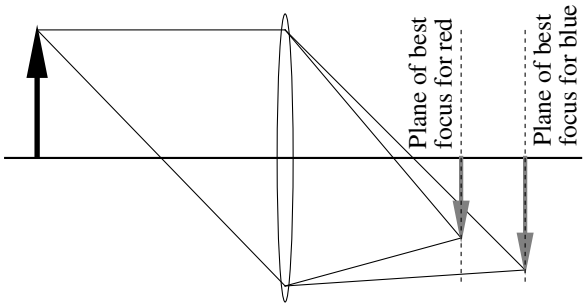

Figure 9: Chromatic aberration

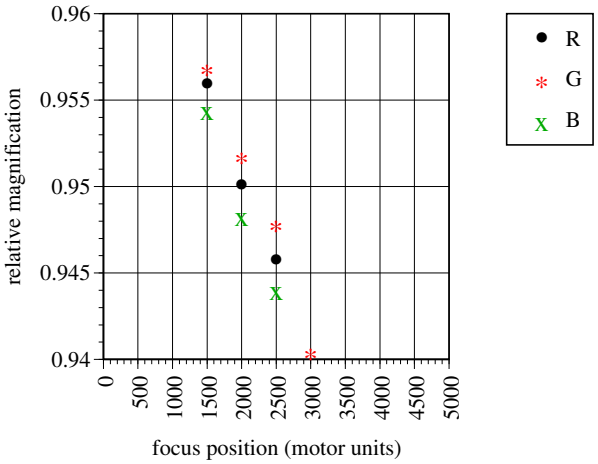

Figure 10: Magnification vs focus distance and color band

3.2 Building a MDOF focussed distance model

The focussed distance of a lens is the distance between the first principle point of the lens and the plane of best focus in object space. For our purposes this definition is not that convenient as the first principle point is a virtual point and not a physical point in the lens. Moreover, the position of the first principle point relative to the camera's coordinate frame can vary as the focal length or the focus of the lens is varied. We prefer to define the focussed distance of the lens as the distance between the plane of best focus in object space and a fixed point in the camera's coordinate frame - usually the sensor plane.

In all imaging systems the sensing plane has a certain finite spatial resolution which gives rise to a zone called the depth of field in which all objects appear to be in focus. There is no distinct plane of best focus. To deal with this we define the focussed distance of a lens to be the distance between a target and the camera's sensor plane at which the target's sharpness (as measured by a sharpness criterion function) peaks. Many sharpness criterion functions have been proposed for machine vision systems [4]. For our work we use the common sum of squared image gradients as a sharpness criterion function.

To a first order approximation the focussed distance of a fixed focal length lens can be controlled by varying the physical distance between the lens and the sensing plane of the camera[1]. Typically researchers have based their focussed distance models on the the thin lens model illustrated in Figure 6 [1], [4]. If we use the thin lens model as the underlying image formation process the focussed distance (as we've defined it) can be expressed mathematically as

$$D = \frac{f_d^2}{f_d - f_l} = g_D(f_l, f_d)$$

where

D	is the distance between the plane of best focus in object space and the sensor plane,
g_D	is the parameterized model of the control parameters,
f_l	is the focal length and
f_d	is the focus (ie. the lens to sensor separation).

According to this model the focussed distance of the lens should be a function of the focal length setting of the lens as well as the focus setting. But modern zoom lenses are typically designed to be equifocal - that is the focussed distance of the lens is designed to remain constant as the focal length of the lens is varied. This represents fundamental inconsistency between our first order lens model and the real behavior of the lens. Without a reasonable idea of the underlying physical process involved to guide us we must now necessarily take a more general modeling approach.

In spite of the equifocal design of the zoom lens, if we take careful measurements of the focussed distance of the lens as the focal length is varied we find, as shown in Figure 11, that the focussed distance of the lens does indeed vary with changes in the lens' focal length, although not to the degree that our first order model would suggest. As a result the focal length parameter will have to be included in the focussed distance model.

In a zoom lens the position of the plane of best focus should be unaffected by changes in the lens' aperture. Again though, if we take careful measurements we find that the position of sharpest focus for the lens is also a function of the lens aperture. Figure 12 shows the variation

[1] For variable focal length lenses the process is conceptually the same.

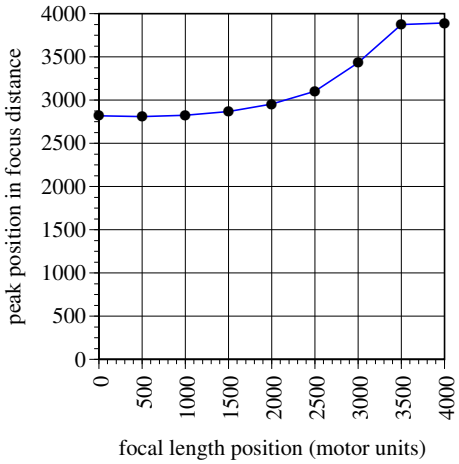

Figure 11: Peak focus position vs focal length

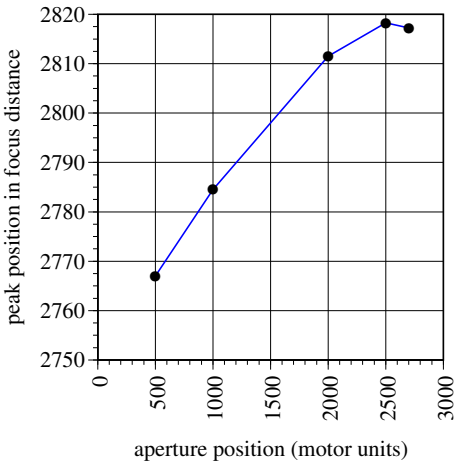

Figure 12: Peak focus position vs aperture

in the sharpest focus motor position with changes in the lens aperture. Part of this variation may be due to the effects of asymmetric changes in the depth of field with aperture, and part of the variation may be due to spherical aberration within the lens. In either event the aperture parameter will need to be included in the model.

Checking out the final DOF, the camera's color band, we find that like the magnification model the focussed distance of the lens is in fact influenced by the wavelength of the light used in imaging. This difference in focussed distance is the result of longitudinal chromatic aberration, illustrated in Figure 9. So, like our MDOF magnification model, the focussed distance model must also be parameterized with the color band. In the end our final 4-DOF focussed distance model has the form

$$D = g_D(f_l, f_d, a, \lambda; c_1 ... c_n)$$

where

D	is the focussed distance,
g_D	is the parameterized model of the control parameters and calibration constants,
f_l	is the focal length motor,
f_d	is the focus motor,
a	is the aperture motor,
λ	is the color band and
$c_1 ... c_n$	are coefficients determined by calibration.

3.3 Building a MDOF optical axis model

The optical axis of a camera system is defined as the line passing through the centers of the optical elements of the camera system. In front of the lens the optical axis points to the focus of expansion or center of perspective in the scene being imaged. Behind the lens the optical axis intersects the sensing plane at the image center.

To a first order approximation the optical axis of a camera system is simply a function of the camera's position and orientation parameters, x, y, z, θ_x, θ_y and θ_z. As the kinematics of

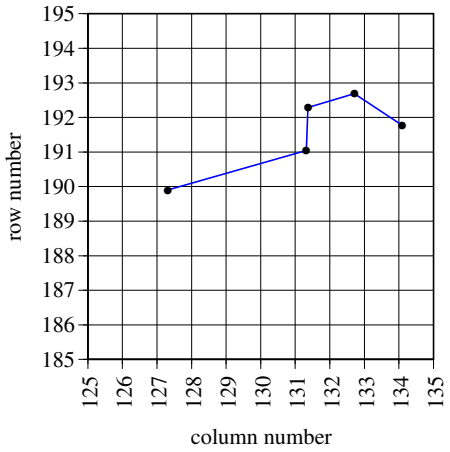

Figure 13: Image center for 5 focus distances

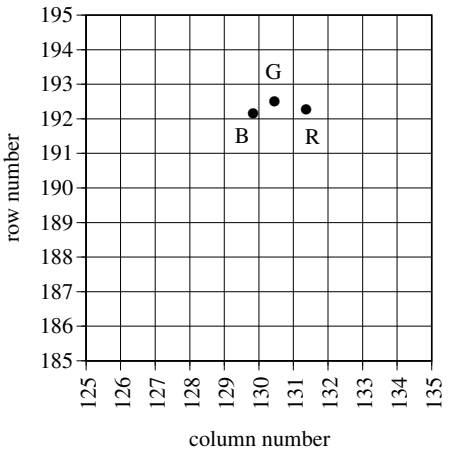

Figure 14: Image center for 3 image bands

the camera's positioning system are in general easily accessible there is usually not much of a problem determining the form of the mathematical model g_A for the optical axis. The resulting 6-DOF model has the form

$$A = g_A(m_1 ... m_6; c_1 ... c_n)$$

where

A	is the optical axis vector,
g_A	is the parameterized model of the control parameters and calibration constants,
$m_1 ... m_6$	are the settings of the camera's positioning motors and
$c_1 ... c_n$	are coefficients determined by calibration.

Many researchers have observed though that the lens's image center shifts in the order of several pixels as the focus distance and focal length parameters of camera lens's are varied [5], [3], [7]. Figure 13 shows the relative drift in the sensor plane of the camera's image center as the focal length of the lens is varied. It has also been shown [8] that the effects of chromatic aberration can result in differences in the image centers between separate color image bands in the order of half a pixel. Figure 14 shows the relative position of the camera's center of perspective for the red image bands for five focus distance settings. The physical process responsible for this drift is the unavoidable misalignment of the optical components on the lens that results from manufacturing tolerances. Changing the positions of lens components relative to the sensing plane, either by adjusting the focus or the focal length, causes changes in the misalignment which in turn causes the image center to move. In addition, the slightly different optical paths through the lens taken by light of different wavelengths means that for any given lens position each image band will not necessarily have the same optical axis. Since measurement and modeling of the misalignment of the optical components is virtually impossible, we are again forced to augment the optical axis model using generic modeling techniques. In the end our 9-DOF model for the optical axis will have the form

$$A = g_A(m_1 ... m_6, f_l, f_d, \lambda; c_1 ... c_n)$$

where

A	is the description of the optical axis vector,
g_A	is the parameterized model of the control parameters and calibration constants,
$m_1 ... m_6$	are the settings of the camera's positioning motors,
f_l	is the focal length motor,
f_d	is the focus motor,
λ	is the color band and
$c_1 ... c_n$	are coefficients determined by calibration.

3.4 The general calibration approach

In the above sections our objective has been to develop and calibrate mathematical models that describe how specific image parameters are influenced by the camera control parameters. In the general case we end up with a model of some image parameter X, expressed as a function of the set of camera control parameters and a set of calibration constants, eg:

$$X = g_X(f_l, f_d, a, \lambda, m_1 ... m_6; c_1 ... c_n)$$

The CIL camera system has 6 position and orientation DOFs, 3 lens DOFs and 1 image band DOF - giving the control space for the system a dimensionality of 10. If we assume nothing about the underlying physical processes responsible for g_X then blindly trying to model the relationship between the control parameters and the parameters of the resulting image is useless. The dimensionality of the system is too high. Instead, a better approach is to start by trying to model the effects of the most significant control parameter. Using measurements of the image parameter as the control parameter is varied we obtain a data set that can be used to calculate the calibration coefficients of the model. The data set and the model are of the same dimensionality. Once the model's form has been adjusted and calibrated so that it faithfully predicts the image parameter's behavior, we increase the dimensionality of the data by taking new measurements while varying an additional control parameter. If the data shows a dependence on the new parameter we add the new parameter to the model and try different model forms until the new data is faithfully reproduced. The process of testing new parameters and adding them to the model continues until we've covered the entire parameter space for the system.

Three issues arise here. The first is which order we should test the control parameters. For any given image parameter the importance of each control parameter varies. Image magnification for example is primarily a function of the lens' focal length. The focus distance and image band have only second order effects on the magnification and should be modeled only after the focal length parameter. At the other end of the scale the camera system's position and orientation control parameters have no bearing on the magnification parameter and need not be tested at all.

The second issue is the determination of the form of the model's equations. The first order effects on an image parameter by the most important control parameters can often be described by using a simplified understanding of the underlying physical processes involved. Thus the form of the first order model is often easy to come by. However, as we progress from first order effects to more subtle ones we see our certainty in the form of the model diminish to the point where we can no longer come up with good model forms based on underlying physical processes - either the underlying processes are too complex to capture in a simple model or they are just not understood well enough. In either case to handle the problem we must resort to

more general modeling techniques. What if calibration reveals that no one function can model g_X over the entire range of the control parameters? Then we may have to resort to several piecewise patches of g_X, with coefficients $(c_1 ... c_n)$ for each patch and some kind of interpolation or blending functional.

A third issue in modeling the camera's behavior is how complex to make the models. For the magnification model we chose a 10 coefficient bivariate cubic polynomial to model the relationship between the magnification and the focus and focal length. By choosing higher order polynomials we can theoretically obtain better fits between the model and the calibration data. In reality though, the data used to calibrate the models is the product of both the underlying physical processes and measurement errors. If our models are too simple they will be unable to capture the full behavior of the underlying physical process. If they are too complex they may capture variations in the data that are really due to measurement noise. As a pragmatic approach the complexity of the model need only be increased to the point at which additional model complexity no longer improves the performance of the task for which the model is being used.

We have noted two particular situations in which the simplest first order or 1-DOF models of the M, D and A image parameters are inadequate for common vision tasks - chromatic aberration and focus magnification. For both cases, by developing more detailed models, we have been able to find a way to control the lens to achieve better image quality and better results in the vision tasks. We now present those problems and their solution.

4 MDOF camera models and machine vision tasks

Many vision tasks make use of sequences of images taken while one of the control parameters in the imaging system is varied. For example, in color image analysis typically three images of the same scene are taken in three different color bands by changing the filter in front of the camera. In focus ranging sequences of images are taken at different focussed distances by varying the lens' focus parameter. In these tasks there is usually an underlying assumption about the relationship between the changes in the camera's parameters and the changes in the parameters of the resulting images. For the most part these assumptions are based on first order approximations of the lens behaviour.

In this section we illustrate how the assumption of first order lens behavior causes problems for both the color image analysis and focus ranging tasks. Subsequently we show how taking into account the second order lens behaviors by using MDOF models we can significantly improve the performance of the tasks.

4.1 MDOF color imaging

Color image analysis uses the information contained in three spectral bands to determine properties of the scene being imaged. Implicit in any color image analysis is the assumption that the per pixel information in each band corresponds to the same point, region, or volume in object space. As we will demonstrate in the following section, this is not always so.

In traditional still color imaging the sequence of images is taken by varying a single DOF - the color band (ie. filter). To a first order approximation we expect that since the focus, zoom, aperture, position and orientation of the camera are unchanged then the focussed distance, magnification and optical axis of the three images will also be unchanged. As we have described in the previous section though, this first order approximation of the lens behavior is not necessarily that good. In this case the second order effect of chromatic aberration causes significant magnification, focus, and centering differences between each of the imaging bands.

Instead of the 1-DOF color imaging approach, if we use the MDOF camera models g_M, g_D and g_A we can determine the control parameter values required to take images that have the same magnification, focussed distance and image center. Given the parameter values for the blue image $(f_{l_b}, f_{d_b}, a_b, \lambda_b, m_{1_b} ... m_{6_b})$, we can find the correct parameter values for the red and green images by satisfying the following constraints:

$$g_M(f_{l_r}, f_{d_r}, \lambda_r) = g_M(f_{l_g}, f_{d_g}, \lambda_g) = g_M(f_{l_b}, f_{d_b}, \lambda_b),$$

$$g_D(f_{l_r}, f_{d_r}, a_b, \lambda_r) = g_D(f_{l_g}, f_{d_g}, a_b, \lambda_g) = g_D(f_{l_b}, f_{d_b}, a_b, \lambda_b),$$

$$g_A(m_{1_r} ... m_{6_r}, f_{l_r}, f_{d_r}, a_b, \lambda_r) = g_A(m_{1_g} ... m_{6_g}, f_{l_g}, f_{d_g}, a_b, \lambda_g) = g_A(m_{1_b} ... m_{6_b}, f_{l_b}, f_{d_b}, a_b, \lambda_b)$$

The following table lists a typical set of control parameter values for a corrected set of color images taken using the Cosmicar/Panasonic camera system.

band	focus motor (out of 3900)	difference from blue setting	focal length motor (out of 4000)	difference from blue setting	camera x shift
red	1407	-6.36%	533	+0.83%	0.006 in
green	1592	-1.62%	508	+0.20%	0.002 in
blue	1655		500		

One thing to note in this table is the fine level of control required to correct for the magnification and centering differences between the color bands. In contrast the variation in the focus motor positions required to equalize the focussed distance is very large.

To determine the effectiveness of the MDOF color imaging approach we measure the misregistration between the image bands of a color picture of a black on white checkerboard test target. The basic procedure involves accurately locating the positions of the checkerboard's black to white step edges to sub pixel accuracy in each of the bands. The relative positions of the same black to white edges in each band then provide a measure of the chromatic aberration induced misregistration at that position in the image. By using a dense set of vertical and horizontal black to white edges (eg. the checkerboard pattern) we can approximate the misregistration at any point in the image by using the nearest pairs of horizontal and vertical step edges to determine the orthogonal components of the misregistration.

Figures 15 and 16 show the magnitude of the image misregistration (in pixel widths) between the blue and red images coded in a gray scale ranging from 0 pixels (black) to 1.5 pixels (white). Figure 15 shows the blue-red misregistration for a set of images taken with the 1-DOF approach. The misregistration across the image ranges from 0 to 1.2 pixel widths. For the blue-red case the zero error region appears to the lower right of the center of the image. In general the location of the zero error region for blue-green case will not be the same. Figure 16 shows the magnitude of the blue-red misregistration for a set of images taken with the MDOF approach. In these images the blue-red misregistration is less than 0.1 pixel widths over most of the image. This represents and order of magnitude improvement over the conventional single DOF approach.

4.2 MDOF focus ranging

In focus ranging the distance to a feature in the camera's field of view is estimated by moving the camera lens through a series of focus positions while determining the sharpness of the feature's image at each position. The feature's sharpness is measured using a criterion function evaluated over the image. Given the focus position of the lens where the criterion function peaks, the distance between the camera and the feature in the image can be estimated using a calibrated lens model.

In conventional focus ranging the sequence of images is taken while varying a single DOF - the lens' focus. As we have described in the previous section, varying the focus of the camera's lens causes the second order effect of focus magnification. As described in [8], these changes in image magnification can lead to a target dependent bias in the position of the criterion function peak. This bias error in the position of the criterion function peak which can result in range estimate errors of up to 6%. To eliminate this bias we need to vary the focussed distance of the lens without changing the image magnification. We call this approach Constant Magnification Focusing.

By using the MDOF camera models g_M and g_D we can determine the control parameter values required to take the constant magnification images. Given a starting set of control parameter values f_{l_s}, f_{d_s} and λ_s, we can find a sequence of parameter values for the remaining images by satisfying the following constraint:

$$g_M(f_{l_s}, f_{d_s}, \lambda_s) = g_M(f_{l_1}, f_{d_1}, \lambda_s) = ... = g_M(f_{l_n}, f_{d_n}, \lambda_s),$$

where the values of f_{d_i} are chosen by some focus search strategy. This represents a new 2-DOF approach to focus ranging, in contrast to the traditional single DOF approach.

Having found the lens control parameters at which the criterion function peaks we simply use the focussed distance model g_D to determine the feature's range. Note that we actually

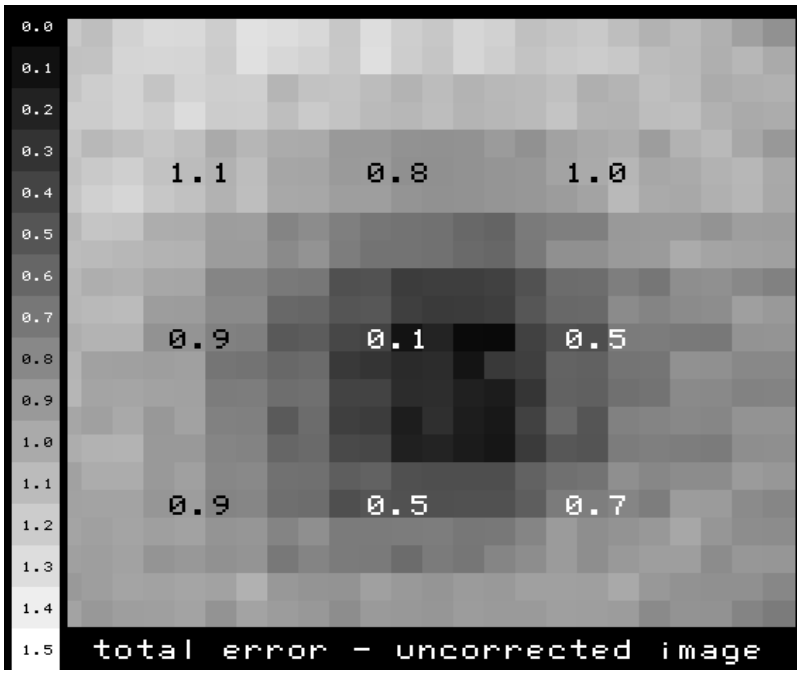

Figure 15: Full field error - conventional (1-DOF) imaging approach

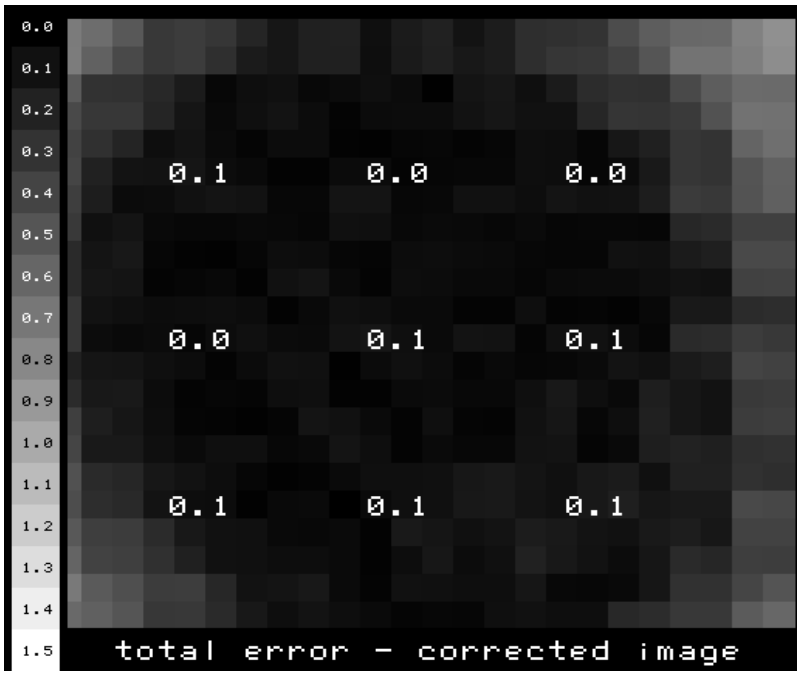

Figure 16: Full field error - MDOF imaging approach

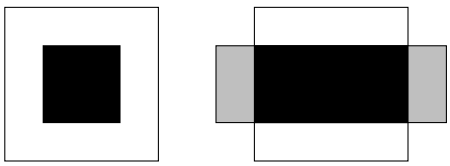

Figure 17: Box and bar focus targets

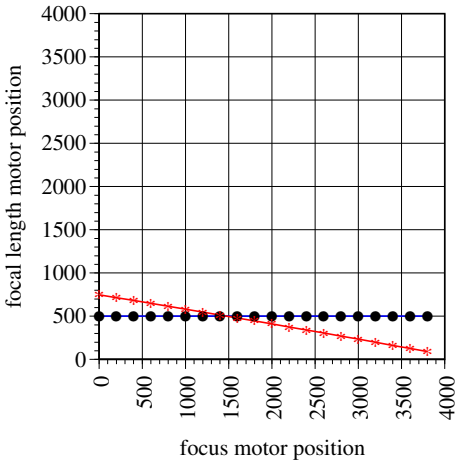

Figure 18: Focus vs focal length settings for MDOF focusing

require two MDOF camera models, g_M and g_D for the MDOF focus ranging approach. The first model is required to implement Constant Magnification Focusing. The second model is required because with Constant Magnification Focusing the criterion function peak will be found at a unique focus distance and focal length position.

To illustrate the effects of focus magnification on the position of the Tenengrad criterion function peak we use two targets, illustrated in Figure 17. Target 1 is a black square on a white background, completely enclosed in the evaluation window. Target 2 is a black bar on a white background with only the center region of the bar contained in the evaluation window. For both targets, the majority of the value of the criterion function results from the black to white edge, with the totally white and totally black regions contributing insignificant amounts. For target 1 the length of the perimeter of the black region changes with the focus magnification, while for target 2 the perimeter length remains constant. The box and bar targets are both located on the same plane exactly 1.5m $\pm$5mm away from the camera's sensor plane.

For the conventional 1-DOF focusing the focussed distance motor is varied while the focal length motor is held constant at 500 motor units ($f_l \approx 67$mm). The image magnification over the range of focus changes by a factor of 0.751. For MDOF Constant Magnification Focusing the focussed distance motor is varied while the focal length motor is concurrently varied to keep the magnification constant. Figure 18 shows the focal length motor settings versus the focussed distance motor settings for both the compensated and the uncompensated focusing. For compensated focusing the focal length motor settings are varied from 747 motor units ($f_l \approx 63$mm) to 91 motor units ($f_l \approx 73$mm). The Constant Magnification Focusing curve is essentially an isomagnification contour from the magnification model shown in Figure 8.

Figure 19 shows that with conventional focusing there is a significant bias in the peak position for the box. When the focus magnification is compensated for, the bias in the peak position for the box target is eliminated. The peak position for the bar target is unaffected. With an actual range of 1.5m, the bias in the uncompensated box target's peak position corresponds to a 6% error in the range measurement determined from the calibrated lens model.

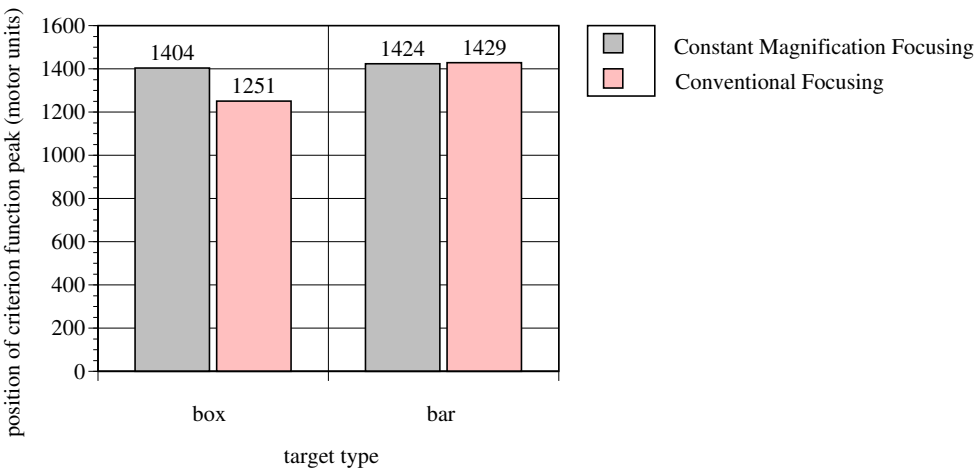

Figure 19: Criterion function peak position vs target type and focus type

5 Conclusions

First order camera models for image parameters cannot capture significant second order effects in lens behavior, and are thus of limited use in multi degree of freedom camera systems. To more effectively use multi degree of freedom camera systems we need to have accurate calibrated models describing the influence of all of the camera's control parameters on each individual image parameter. With these models it is possible to significantly improve the performance of low level vision tasks.

In the modeling process as we progress from the first order effects to more subtle second order effects we see our certainty in the form of the model diminish to the point where we can no longer come up with good model forms based on underlying physical processes - either the underlying processes are too complex to capture in a simple model or they are just not understood well enough. In either case we must resort to more general modeling techniques to deal with the situation.

The development of multi degree of freedom camera models requires extensive experimentation to determine the significant parameters for the models, to determine the forms of the models, and to obtain calibration data.

To perform the experiments needed to validate and develop the model forms and to obtain calibration data for the models we need precise automated imaging systems.

6 Acknowledgments

This research was sponsored by the Avionics Laboratory, Wright Research and Development Center, Aeronautical Systems Division (AFSC), U. S. Air Force, Wright-Patterson AFB, OH 45433-6543 under Contract F33615-90-C-1465, ARPA Order No. 7597.

The views and conclusions contained in this document are those of the authors and should not be interpreted as representing the official policies, either expressed or implied, of DARPA or the U.S. Government.

References

[1] A. L. Abbott. *Dynamic Integration of Depth Cues for Surface Reconstruction From Stereo Images*. PhD thesis, University of Illinois at Urbana-Champaign, January 1991.

[2] H. A. Beyer. Linejitter and geometric calibration of ccd-cameras. *ISPRS Journal of Photogrammetry and Remote Sensing*, 45(1):17–32, 1990.

[3] T. Darrell and K. Wohn. Pyramid based depth from focus. In *Proceedings of Computer Vision and Pattern Recognition*, pages 504–509, Ann Arbor, Michigan, June 1988. Computer Society, IEEE Computer Society.

[4] E. P. Krotkov. Exploratory visual sensing for determining spatial layout with an agile stereo camera system. PhD Thesis MS-CIS-87-29, University of Pennsylvania, April 1987.

[5] R. K. Lenz and R. Y. Tsai. Techniques for calibration of the scale factor and image center for high accuracy 3d machine vision metrology. In *Proceedings of IEEE International Conference on Robotics and Automation*, pages 68–75, Raleigh, NC, March 1987.

[6] K. Tarabanis and R. Y. Tsai. Model-based planning of sensor placement and optical settings. Technical Report CUCS 502-89, Columbia University, 1989.

[7] A. G. Wiley. *Metric Aspects of Zoom Vision*. PhD thesis, University of Illinois at Urbana-Champaign, June 1991.

[8] R. G. Willson and S. A. Shafer. Dynamic lens compensation for active color imaging and constant magnification focusing. Technical Report CMU-RI-TR-91-26, Carnegie Mellon University, November 1991.

[9] R. G. Willson and S. A. Shafer. Precision imaging and control for machine vision research at carnegie mellon university. In *Proceedings of SPIE Conference on High Resolution Sensors and Hybrid Systems*, San Jose, California, February 1992.